Amplitude Analysis of $B^{\pm} \to \pi^{\pm} K^{+} K^{-}$ Decays

R. Aaij *et al.*[*]
(LHCb Collaboration)

(Received 12 June 2019; revised manuscript received 15 October 2019; published 6 December 2019)

The first amplitude analysis of the $B^{\pm} \to \pi^{\pm} K^{+} K^{-}$ decay is reported based on a data sample corresponding to an integrated luminosity of 3.0 fb^{-1} of pp collisions recorded in 2011 and 2012 with the LHCb detector. The data are found to be best described by a coherent sum of five resonant structures plus a nonresonant component and a contribution from $\pi\pi \leftrightarrow KK$ S-wave rescattering. The dominant contributions in the $\pi^{\pm} K^{\mp}$ and $K^{+} K^{-}$ systems are the nonresonant and the $B^{\pm} \to \rho(1450)^{0} \pi^{\pm}$ amplitudes, respectively, with fit fractions around 30%. For the rescattering contribution, a sizable fit fraction is observed. This component has the largest CP asymmetry reported to date for a single amplitude of $(-66 \pm 4 \pm 2)\%$, where the first uncertainty is statistical and the second systematic. No significant CP violation is observed in the other contributions.

DOI: 10.1103/PhysRevLett.123.231802

Charge-parity (CP) symmetry is known to be broken in weak interactions. In two-body charged B-meson decays, the only CP-violating observable is the difference of the partial decay widths for particle and antiparticle over their sum. For three- and multibody processes, the decay dynamics is very rich, thanks to possible interfering intermediate resonant and nonresonant amplitudes, and therefore CP violation (CPV) can be manifested as charge asymmetries that may vary and even change sign throughout the different regions of the observed phase space.

Several experiments have reported sizable localized CP asymmetries in the phase space of charmless three-body $B^{\pm}$ decays [1–7]. The $B^{\pm} \to \pi^{\pm}\pi^{+}\pi^{-}$ and $B^{\pm} \to \pi^{\pm} K^{+} K^{-}$ decays, having the same flavor quantum numbers, are coupled by final-state strong interactions, in particular through the rescattering process $\pi^{+}\pi^{-} \leftrightarrow K^{+}K^{-}$. The $B^{\pm} \to \pi^{\pm}\pi^{+}\pi^{-}$ decay, with 3 times larger branching fraction, may proceed through resonances from $b \to u$ ($\bar{b} \to \bar{u}$) tree transitions as well as from the $b \to d$ ($\bar{b} \to \bar{d}$) loop-induced penguin processes. On the other hand, the production of resonances in the $B^{\pm} \to \pi^{\pm} K^{+} K^{-}$ decay is limited: $\pi^{\pm} K^{\mp}$ resonances can only be obtained from penguin transitions; $K^{+}K^{-}$ resonances can come from tree-level transitions, but with the $s\bar{s}$ contribution highly suppressed by the OZI rule [8–10]. In the $B^{\pm} \to \pi^{\pm} K^{+} K^{-}$ decay, no significant $\phi(1020) \to K^{+}K^{-}$ contribution has been seen [11]. However, a concentration of events is observed just above the $\phi(1020)$ region in the $K^{+}K^{-}$ invariant-mass spectrum. This corresponds to the region where the S-wave $\pi^{+}\pi^{-} \leftrightarrow K^{+}K^{-}$ rescattering effect is seen, as shown by elastic scattering experiments [12,13]. Intriguingly, in this same region, large CP asymmetries have been observed [1,14]. As proposed in Refs. [15,16], this could be a manifestation of CPV arising from amplitudes with different rescattering strong phases as well as different weak phases.

A better understanding of the CPV mechanisms occurring in three-body hadronic B decays can be achieved through full amplitude analyses. In this Letter, the first amplitude analysis of the decay $B^{\pm} \to \pi^{\pm} K^{+} K^{-}$ is performed based on a data sample corresponding to an integrated luminosity of 3.0 fb^{-1} collected in 2011 and 2012. The isobar model formalism [17,18], which assumes that the total decay amplitude is a coherent sum of intermediate two-body states, is applied. A rescattering amplitude is also included. The magnitudes and phases of the coupling to intermediate states are determined independently for $B^{+} \to \pi^{+} K^{-} K^{+}$ and $B^{-} \to \pi^{-} K^{+} K^{-}$ decays, allowing for CP violation.

The LHCb detector is a single-arm forward spectrometer covering the pseudorapidity range $2 < \eta < 5$ equipped with charged-hadron identification detectors, calorimeters, and muon detectors; and it is designed for the study of particles containing b or c quarks [19,20].

Simulated samples, needed to determine the signal efficiency as well as for background studies, are generated using PYTHIA [21] with a specific LHCb configuration [22]. Decays of hadronic particles are described by EVTGEN [23], in which final-state radiation is generated using PHOTOS [24]. The interaction of the generated particles with the detector and its response are implemented using the GEANT4 toolkit [25] as described in Ref. [26].

[*]Full author list given at the end of the article.

In a preselection stage, $B^{\pm}$ candidates are reconstructed by requiring three charged tracks forming a good-quality secondary vertex, with loose requirements imposed on their momentum, transverse momentum, and impact parameter with respect to any primary vertex. The momentum vector of the B candidate should point back to a primary vertex, from which the $B^{\pm}$ vertex has to be significantly separated. To remove contributions from charm decays, candidates for which the two-body invariant masses $m(K^{\pm}\pi^{\mp})$ and $m(K^{+}K^{-})$ are within 30 MeV$/c^2$ of the known value of the D^0 mass [27] are excluded.

A multivariate selection based on a boosted decision tree (BDT) algorithm [28,29] is applied to reduce the combinatorial background (random combination of tracks). The BDT is described in Ref. [1]; it is trained using a combination of $B^{\pm} \to h^{\pm}h^{+}h^{-}$ samples of simulated events (where h can be either a pion or a kaon) as signal, and data in the high-mass region $5.40 < m(\pi^{\pm}\pi^{+}\pi^{-}) < 5.58$ GeV$/c^2$ of a $B^{\pm} \to \pi^{\pm}\pi^{+}\pi^{-}$ sample as background. The $B^{\pm} \to \pi^{\pm}\pi^{+}\pi^{-}$ sample is used as a proxy for the combinatorial background because, among the various $B^{\pm} \to h^{\pm}h^{+}h^{-}$ channels, it is the only one whose high mass region is populated just by combinatorial background. The selection requirement on the BDT response is chosen to maximize the ratio $N_S/\sqrt{N_S + N_B}$, where N_S and N_B represent the expected number of signal and background candidates in data, respectively, within an invariant mass window of approximately 40 MeV$/c^2$ around the $B^{\pm}$ mass in the data [1].

Particle identification criteria are used to reduce the crossfeed from other b-hadron decays, in particular $K \leftrightarrow \pi$ misidentification. Muons are rejected by a veto applied to each track [30]. Events with more than one candidate are discarded.

An unbinned extended maximum-likelihood fit is applied simultaneously to the $\pi^{+}K^{-}K^{+}$ and $\pi^{-}K^{+}K^{-}$ mass spectra in order to obtain the total signal yields and the raw asymmetry, defined as the difference of B^{-} and B^{+} signal yields divided by their sum. Three types of background sources are identified: the residual combinatorial background, partially reconstructed decays (mostly from four-body decays) and cross feed from other B-meson decays. The parametrization of cross feed and partially reconstructed backgrounds is performed using simulated samples that satisfy the same selection criteria as the data. From the result of the fit, yields for signal and background sources are obtained [1].

Candidates within the mass region $5.266 < m(\pi^{\pm}K^{+}K^{-}) < 5.300$ GeV$/c^2$, referred to as the signal region, are used for the amplitude analysis. This region contains 2052 ± 102 (1566 ± 84) of B^{+} (B^{-}) signal candidates. The relative contribution from the combinatorial background is 23%, with a charge asymmetry compatible with zero within 1 standard deviation. The main cross feed contamination comes from $B^{\pm} \to K^{\pm}\pi^{+}\pi^{-}$ decays which contribute in 2.7% with a charge asymmetry of 2.5% [1]. Another 0.6% comes from $\phi(1020)$ mesons randomly associated with a pion, with negligible charge asymmetry.

The distributions of the selected $B^{\pm}$ candidates, represented by the Dalitz plot [31] constructed by the squared mass combinations $m^2_{\pi^{\pm}K^{\mp}}$ and $m^2_{K^{+}K^{-}}$, are shown in Fig. 1. The clear differences between the B^{+} and the B^{-} distributions are due to CPV effects [1].

The total $B^{+} \to \pi^{+}K^{-}K^{+}$ decay amplitude $\mathcal{A}$ can be expressed as a function of $m^2_{\pi^{+}K^{-}}$ and $m^2_{K^{+}K^{-}}$ as

$$\mathcal{A}(m^2_{\pi^{+}K^{-}}, m^2_{K^{+}K^{-}}) = \sum_{i=1}^{N} c_i \mathcal{M}_i(m^2_{\pi^{+}K^{-}}, m^2_{K^{+}K^{-}}), \quad (1)$$

where $\mathcal{M}_i(m^2_{\pi^{+}K^{-}}, m^2_{K^{+}K^{-}})$ is the decay amplitude for an intermediate state i. The analogous amplitude for the B^{-} meson $\overline{\mathcal{A}}$ is written in terms of $\bar{c}_i$ and $\overline{\mathcal{M}}_i(m^2_{\pi^{-}K^{+}}, m^2_{K^{+}K^{-}})$. This description for the total decay amplitude is known as the isobar model. In the amplitude fit, the complex coefficients $c_i = (x_i + \Delta x_i) + i(y_i + \Delta y_i)$ and $\bar{c}_i = (x_i - \Delta x_i) + i(y_i - \Delta y_i)$ measure the relative contribution of each intermediate state i for B^{+} and B^{-}, respectively, with Δx_i and Δy_i being the parameters that allow for CPV. The individual amplitudes are described by

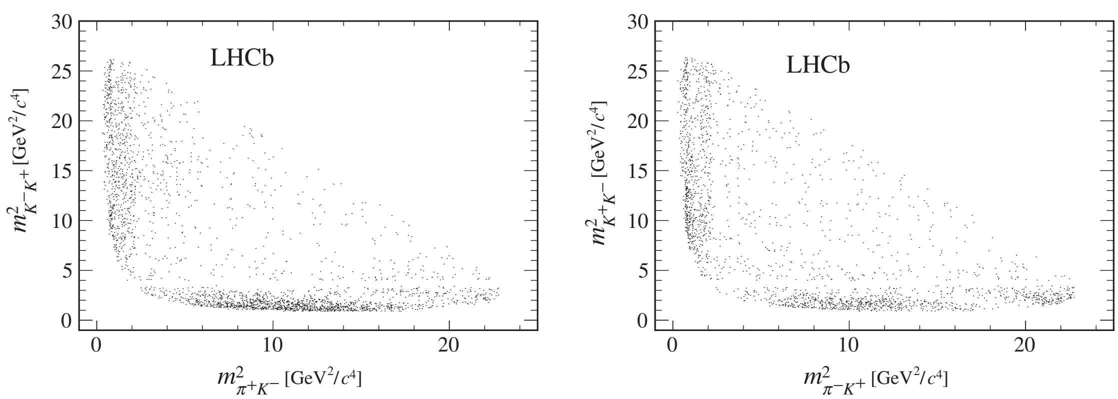

FIG. 1. Dalitz plot for (left) $B^{+} \to \pi^{+}K^{-}K^{+}$ and (right) $B^{-} \to \pi^{-}K^{+}K^{-}$ candidates in the selected signal region.

$$\mathcal{M}_i(m^2_{\pi^+K^-}, m^2_{K^+K^-}) = P_i(J, \vec{p}, \vec{q})F_B(|\vec{p}|)F_i(|\vec{q}|)T_i. \qquad (2)$$

The factor P_i represents the angular part, which depends on the spin J of the resonance. It is equal to 1, $-2\vec{p}\cdot\vec{q}$, and $\frac{4}{3}[3(\vec{p}\cdot\vec{q})^2 - (|\vec{p}||\vec{q}|)^2]$, for $J = 0$, 1, and 2, respectively; $\vec{q}$ is the momentum of one of the resonance decay products and $\vec{p}$ is the momentum of the particle not forming the resonance, both measured in the resonance rest frame. The Blatt-Weisskopf barrier factors [32,33], F_B for the B meson and F_i for the resonance i, account for penetration effects due to the finite extent of the particles involved in the reaction. They are given by 1, $\sqrt{(1+z_0^2)/(1+z^2)}$, and $\sqrt{(z_0^4+3z_0^2+9)/(z^4+3z^2+9)}$ for $J = 0$, 1, and 2, respectively, with $z = |\vec{q}|d$ or $z = |\vec{p}|d$ and d the penetration radius, taken to be 4.0 $(\mathrm{GeV}/c)^{-1} \approx 0.8$ fm [34,35]. The value of z is z_0 when the invariant mass is equal to the nominal mass of the resonance. Finally, T_i is a function representing the propagator of the intermediate state i. By default a relativistic Breit-Wigner function [36] is used, which provides a good description for narrow resonances such as $K^*(892)^0$. More specific line shapes are also used, as discussed further below.

To determine the intermediate state contributions, a maximum-likelihood fit to the distribution of the $B^\pm \to \pi^\pm K^+K^-$ candidates in the Dalitz plot is performed using the LAURA^{++} package [37,38]. The total probability density function (PDF) is a sum of signal and background components, with relative contributions fixed from the result of the $B^\pm \to \pi^\pm K^+K^-$ mass fit. The background PDF is modeled according to its observed structures in the higher $m(\pi^\pm K^+K^-)$ sideband, the contribution from $B^\pm \to K^\pm\pi^+\pi^-$ cross feed decays, using the model introduced by the *BABAR* Collaboration [6], and an additional 0.6% relative contribution from $\phi(1020)$ mesons randomly associated with a pion. The signal PDF for B^+ (B^-) decays is given by $|\mathcal{A}|^2$ ($|\bar{\mathcal{A}}|^2$) multiplied by a function describing the variation of efficiency across the Dalitz plot. A histogram representing this efficiency map is obtained from simulated samples with corrections to account for known differences between data and simulation. The B^+ and B^- candidates are simultaneously fitted, allowing for CP violation. The CP asymmetry A_{CP_i} and fit fraction FF_i for each component are given by

$$A_{CP_i} = \frac{|\bar{c}_i|^2 - |c_i|^2}{|\bar{c}_i|^2 + |c_i|^2} = \frac{-2(x_i\Delta x_i + y_i\Delta y_i)}{x_i^2 + (\Delta x_i)^2 + y_i^2 + (\Delta y_i)^2}, \qquad (3)$$

$$\mathrm{FF}_i = \frac{\int(|c_i\mathcal{M}_i|^2 + |\bar{c}_i\bar{\mathcal{M}}_i|^2)dm^2_{\pi^\pm K^\mp}dm^2_{K^+K^-}}{\int(|\mathcal{A}|^2 + |\bar{\mathcal{A}}|^2)dm^2_{\pi^\pm K^\mp}dm^2_{K^+K^-}}. \qquad (4)$$

The contribution of the possible intermediate states in the total decay amplitude is tested through a procedure in which each component is taken in and out of the model, and that which provides the best likelihood is then maintained, and the process is repeated. In some regions of the phase space the observed signal yields could not be well described with only known resonance states and line shapes, and thus alternative parametrizations were also tested.

In the $\pi^\pm K^\mp$ system, a nonresonant amplitude involving a single-pole form factor of the type $[1 + m^2(\pi^\pm K^\mp)/\Lambda^2]^{-1}$, as proposed in Ref. [14], is included. This component, hereafter called single-pole amplitude, is a phenomenological description of the partonic interaction. The parameter Λ sets the scale for the energy dependence and the proposed value of 1 GeV/c^2 is used.

In the K^+K^- system, a dedicated amplitude accounting for the $\pi\pi \leftrightarrow KK$ rescattering is used. It is expressed as the product of the nonresonant single-pole form factor described above and a scattering term that accounts for the S-wave $\pi\pi \leftrightarrow KK$ transition amplitude, with isospin equal to 0 and $J = 0$, given by the off-diagonal term in the S matrix for the $\pi\pi$ and KK coupled channel. The scattering term is expressed as $\sqrt{1-\nu^2}e^{2i\delta}$, where the inelasticity (ν) and phase shift (δ) parametrizations are taken from Ref. [39]. For the mass range 0.95 to 1.42 GeV/c^2, where the coupling $\pi\pi \to KK$ is known to be important, these parameters are given by

$$\nu = 1 - \left(\epsilon_1\frac{k_2}{s^{1/2}} + \epsilon_2\frac{k_2^2}{s}\right)\frac{M'^2 - s}{s} \qquad (5)$$

and

$$\cot\delta = C_0\frac{(s - M_s^2)(M_f^2 - s)}{M_f^2 s^{1/2}}\frac{|k_2|}{k_2^2}, \qquad (6)$$

with parameters set as given in Ref. [39].

For all models tested in the analysis, the channel $B^\mp \to \overset{(-)}{K}{}^*(892)^0K^\mp$ is used as reference, with its real part x fixed to one, y and Δy fixed to zero, while Δx is free to vary. The values of x, y, Δx, and Δy for all other contributions are free parameters. The masses and widths of all resonances are fixed [27].

The fit results are summarized in Table I. Seven components are required to provide an overall good description of data; three of them correspond to the structure in the $\pi^\pm K^\mp$ system, and four for the K^+ K^- system. Statistical uncertainties are derived from the fitted values of x, y, Δx, Δy, with correlations and error propagation taken into account; sources of systematic uncertainty are also evaluated as described later.

The $\pi^\pm K^\mp$ system is well described by the contributions from the $K^*(892)^0$ and $K_0^*(1430)^0$ resonances plus the single-pole amplitude. The inclusion of the latter provides a better description of the data than that obtained from the $K_0^*(700)$, $K_2^*(1430)^0$, $K^*(1410)^0$, and $K^*(1680)^0$ resonances. The largest contribution is from the single-pole

TABLE I. Results of the Dalitz plot fit, where the first uncertainty is statistical and the second systematic. The fitted values of c_i ($\bar{c}_i$) are expressed in terms of magnitudes $|c_i|$ ($|\bar{c}_i|$) and phases $\arg(c_i)$ [$\arg(\bar{c}_i)$] for each B^+ (B^-) contribution. The top row corresponds to B^+ and the bottom to B^- mesons.

Contribution	Fit fraction (%)	A_{CP} (%)	Magnitude (B^+/B^-)	Phase [°] (B^+/B^-)
$K^*(892)^0$	$7.5 \pm 0.6 \pm 0.5$	$+12.3 \pm 8.7 \pm 4.5$	$0.94 \pm 0.04 \pm 0.02$	0 (fixed)
			$1.06 \pm 0.04 \pm 0.02$	0 (fixed)
$K_0^*(1430)^0$	$4.5 \pm 0.7 \pm 1.2$	$+10.4 \pm 14.9 \pm 8.8$	$0.74 \pm 0.09 \pm 0.09$	$-176 \pm 10 \pm 16$
			$0.82 \pm 0.09 \pm 0.10$	$136 \pm 11 \pm 21$
Single pole	$32.3 \pm 1.5 \pm 4.1$	$-10.7 \pm 5.3 \pm 3.5$	$2.19 \pm 0.13 \pm 0.17$	$-138 \pm 7 \pm 5$
			$1.97 \pm 0.12 \pm 0.20$	$166 \pm 6 \pm 5$
$\rho(1450)^0$	$30.7 \pm 1.2 \pm 0.9$	$-10.9 \pm 4.4 \pm 2.4$	$2.14 \pm 0.11 \pm 0.07$	$-175 \pm 10 \pm 15$
			$1.92 \pm 0.10 \pm 0.07$	$140 \pm 13 \pm 20$
$f_2(1270)$	$7.5 \pm 0.8 \pm 0.7$	$+26.7 \pm 10.2 \pm 4.8$	$0.86 \pm 0.09 \pm 0.07$	$-106 \pm 11 \pm 10$
			$1.13 \pm 0.08 \pm 0.05$	$-128 \pm 11 \pm 14$
Rescattering	$16.4 \pm 0.8 \pm 1.0$	$-66.4 \pm 3.8 \pm 1.9$	$1.91 \pm 0.09 \pm 0.06$	$-56 \pm 12 \pm 18$
			$0.86 \pm 0.07 \pm 0.04$	$-81 \pm 14 \pm 15$
$\phi(1020)$	$0.3 \pm 0.1 \pm 0.1$	$+9.8 \pm 43.6 \pm 26.6$	$0.20 \pm 0.07 \pm 0.02$	$-52 \pm 23 \pm 32$
			$0.22 \pm 0.06 \pm 0.04$	$107 \pm 33 \pm 41$

amplitude with a total fit fraction of about 32%. The $K^*(892)^0$ and the $K_0^*(1430)^0$ amplitudes contribute to 7.5% and 4.5%, respectively. Given that they originate from penguin-diagram processes, their contributions to the total rate are expected to be small. The projection of the data onto $m^2_{\pi^\pm K^\mp}$ with the fit model overlaid, is shown in Fig. 2.

In the K^+K^- system, two main signatures can be highlighted: a strong destructive interference localized between 0.8 and 3.3 GeV^2/c^4 in $m^2_{K^+K^-}$ and projected between 12 and 20 GeV^2/c^4 in $m^2_{\pi^\pm K^\mp}$, as shown in Fig. 1; and the large CP asymmetry for $m^2_{K^+K^-}$ corresponding to the $\pi\pi \leftrightarrow KK$ rescattering region, as shown in Fig. 3. For the former, a good description of the data is achieved only when a high-mass vector amplitude is included in the Dalitz plot fit, producing the observed pattern through the interference with the $f_2(1270)$ amplitude. The data are well described by assuming this contribution to be the $\rho(1450)^0$ resonance, included in the fit with mass and width

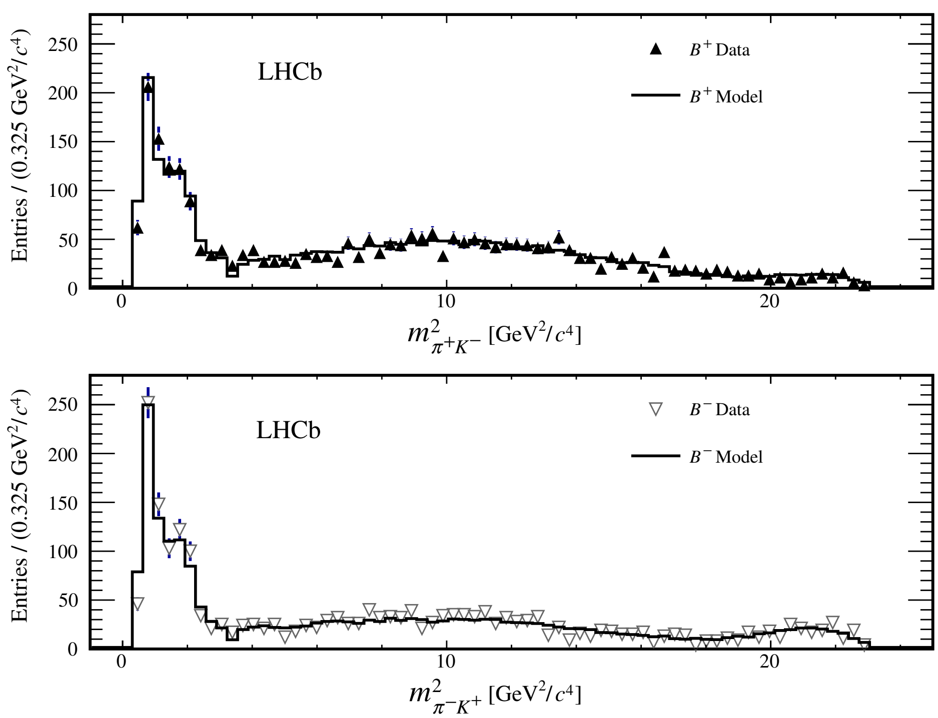

FIG. 2. Distribution of $m^2_{\pi^\pm K^\mp}$. Data are represented by points for B^+ and B^- candidates separately, with the result of the fit overlaid.

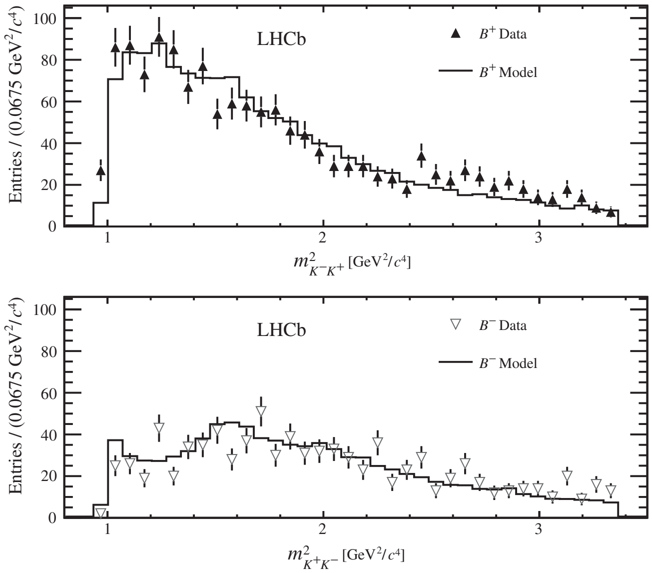

FIG. 3. Distribution of $m^2_{K^+K^-}$ up to 3.5 GeV^2/c^4. Data are represented by points for B^+ and B^- separately, with the result of the fit overlaid.

fixed to their known values [27]. The corresponding $B^\pm \to \rho(1450)^0\pi^\pm$ fit fraction is approximately 30%, a rather large contribution not expected for the K^+K^- pair as the dominant decay mode is $\pi\pi$ and the $\rho(1450)^0$ contribution in $B^\pm \to \pi^\pm\pi^+\pi^-$ is observed to be much lower [40,41]. A future analysis with the addition of the run 2 data recorded with the LHCb detector should be able to better pinpoint this effect.

With respect to the low $m^2_{K^+K^-}$ region, shown in Fig. 3, a significant contribution with a fit fraction of 16% from the $\pi\pi \leftrightarrow KK$ S-wave rescattering amplitude is found. This contribution alone produces a CP asymmetry of $(-66 \pm 4 \pm 2)\%$, which is the largest CPV manifestation ever observed for a single amplitude. This must be directly related to the total inclusive CP asymmetry observed in this channel, which was previously reported to be $(-12.3 \pm 2.1)\%$. For the coupled channel $B^\pm \to \pi^\pm\pi^+\pi^-$, with a branching fraction 3 times larger than that of $B^\pm \to \pi^\pm K^+K^-$, a positive CP asymmetry has been measured [1]. This gives consistency for the interpretation of the large CPV observed here originates from rescattering effects. Finally, the inclusion of the $\phi(1020)$ resonance in the amplitude model also improves the data description near the K^+ K^- threshold, however, with a statistically marginal contribution. The model is also not perfect in other regions in $m^2_{K^+K^-}$, for instance, for B^+ decays in a few bins above 2.5 GeV^2/c^4.

A second solution is found in the fit, presenting a large CP asymmetry of 76% in the $K_0^*(1430)^0$ component, compensated by a similarly large negative asymmetry in the interference term between the $K_0^*(1430)^0$ and the single-pole amplitudes. The net effect is a negligible CP asymmetry near the $K_0^*(1430)^0$ region, matching what is seen in the data. This solution presents a large sum of fit fractions for the B^- decay, of about 130%, indicating this is probably a fake effect created by the fit. As such, this solution is interpreted as unphysical. More data are necessary to understand this feature.

Several sources of systematic uncertainty are considered. These include possible mismodelings in the mass fit, the efficiency variation and background description across the Dalitz plot, the uncertainty associated to the fixed parameters in the Dalitz plot fit and possible biases in the fitting procedure.

The impact of the systematic studies affect differently each of the amplitudes. The main contribution comes from the variation of the masses and widths of the resonances; their central values and uncertainties are taken from Ref. [27] and are randomized according to a Gaussian distribution. This effect is particularly important for the $K_0^*(1430)^0$ and single-pole components, the two broad scalar contributions in the $\pi^\pm K^\mp$ system. The absolute uncertainties on their fractions are found to be 0.8% and 3.0%, respectively. The second main contribution comes from the $\pi^\pm K^+K^-$ mass fit, impacting most on the $K^*(892)^0$, $K_0^*(1430)^0$ and single-pole fractions with uncertainties of 0.4%, 0.8%, and 2.0%, respectively. The systematic uncertainty associated with efficiency variation across the Dalitz plot is studied by performing several fits to data with efficiency maps obtained by varying the bin contents of the original efficiency histogram according to their uncertainty; this results in uncertainties in the fit fractions that range from 0.01% to 0.1%. The systematic uncertainty due to the background models is evaluated with a similar procedure, also resulting in small uncertainties. The $B^\pm$ production and kaon detection asymmetry effects are taken into account following Ref. [42], with associated uncertainties less than 0.1%. All systematic uncertainties are added in quadrature and represent the second uncertainty in Table I.

In summary, the resonant substructure of the charmless three-body $B^\pm \to \pi^\pm K^+K^-$ decay is determined using the isobar model formalism, providing an overall good description of the observed data. Three components are obtained for the $\pi^\pm K^\mp$ system: two resonant states [$K^*(892)^0$, $K_0^*(1430)^0$] with a CP asymmetry consistent with zero, and a nonresonant single-pole form factor contribution with a fit fraction of about 30%. Two other components are found, $\rho(1450)^0$ and $f_2(1270)$, which provide a destructive interference pattern in the Dalitz plot. The rescattering amplitude, acting in the region $0.95 < m(K^+K^-) < 1.42\ \mathrm{GeV}/c^2$, produces a negative CP asymmetry of $(-66 \pm 4 \pm 2)\%$, which is the largest CP violation effect observed from a single amplitude.

We express our gratitude to our colleagues in the CERN accelerator departments for the excellent performance of the LHC. We thank the technical and administrative staff at the LHCb institutes. We acknowledge support from CERN and from the national agencies: CAPES, CNPq, FAPERJ, and FINEP (Brazil); MOST and NSFC (China); CNRS/IN2P3 (France); BMBF, DFG, and MPG (Germany); INFN (Italy); NWO (Netherlands); MNiSW and NCN (Poland); MEN/IFA (Romania); MSHE (Russia); MinECo (Spain); SNSF and SER (Switzerland); NASU (Ukraine); STFC (United Kingdom); DOE NP and NSF (USA). We acknowledge the computing resources that are provided by CERN, IN2P3 (France), KIT, and DESY (Germany), INFN (Italy), SURF (Netherlands), PIC (Spain), GridPP (United Kingdom), RRCKI and Yandex LLC (Russia), CSCS (Switzerland), IFIN-HH (Romania), CBPF (Brazil), PL-GRID (Poland), and OSC (USA). We are indebted to the communities behind the multiple open-source software packages on which we depend. Individual groups or members have received support from AvH Foundation (Germany); EPLANET, Marie Skłodowska-Curie Actions and ERC (European Union); ANR, Labex P2IO, and OCEVU, and Région Auvergne-Rhône-Alpes (France); Key Research Program of Frontier Sciences of CAS, CAS PIFI, and the Thousand Talents Program (China); RFBR, RSF, and Yandex LLC (Russia); GVA, XuntaGal, and GENCAT (Spain); the Royal Society and the Leverhulme Trust (United Kingdom).

[1] R. Aaij *et al.* (LHCb Collaboration), Measurement of CP violation in the three-body phase space of charmless $B^{\pm}$ decays, Phys. Rev. D **90**, 112004 (2014).
[2] C. L. Hsu *et al.* (Belle Collaboration), Measurement of branching fraction and direct CP asymmetry in charmless $B^+ \to K^+K^-\pi^+$ decays at Belle, Phys. Rev. D **96**, 031101 (R) (2017).
[3] B. Aubert *et al.* (*BABAR* Collaboration), Observation of the Decay $B^+ \to K^+K^-\pi^+$, Phys. Rev. Lett. **99**, 221801 (2007).
[4] B. Aubert *et al.* (*BABAR* Collaboration), Dalitz plot analysis of $B^{\pm} \to \pi^{\pm}\pi^{\pm}\pi^{\mp}$ decays, Phys. Rev. D **79**, 072006 (2009).
[5] J. P. Lees *et al.* (*BABAR* Collaboration), Study of CP violation in Dalitz-plot analyses of $B^0 \to K^+K^-K^0_S$, $B^+ \to K^+K^-K^+$, and $B^+ \to K^0_S K^0_S K^+$, Phys. Rev. D **85**, 112010 (2012).
[6] B. Aubert *et al.* (*BABAR* Collaboration), Evidence for direct CP violation from Dalitz-plot analysis of $B^{\pm} \to K^{\pm}\pi^{\mp}\pi^{\pm}$, Phys. Rev. D **78**, 012004 (2008).
[7] A. Garmash *et al.* (Belle Collaboration), Evidence for Large Direct CP Violation in $B^{\pm} \to \rho(770)^0 K^{\pm}$ from Analysis of the Three-Body Charmless $B^{\pm} \to K^{\pm}\pi^{\pm}\pi^{\mp}$ Decay, Phys. Rev. Lett. **96**, 251803 (2006).
[8] S. Okubo, ϕ-meson and unitary symmetry model, Phys. Lett. **5**, 165 (1963).
[9] G. Zweig An SU_3 model for strong interaction symmetry and its breaking; Version 1, Technical Report CERN-TH-401, CERN, Geneva, 1964.
[10] J. Iizuka, Systematics and phenomenology of meson family, Prog. Theor. Phys. Suppl. **37**, 21 (1966).
[11] R. Aaij *et al.* (LHCb Collaboration), Measurement of the charge asymmetry in $B^{\pm} \to \phi K^{\pm}$ and search for $B^{\pm} \to \phi\pi^{\pm}$ decays, Phys. Lett. B **728**, 85 (2014).
[12] P. Estabrooks *et al.*, $\pi\pi$ phase shift analysis from 600 to 1900 MeV, AIP Conf. Proc. **13**, 206 (1973).
[13] D. H. Cohen, D. S. Ayres, R. Diebold, S. L. Kramer, A. J. Pawlicki, and A. B. Wicklund, Amplitude analysis of the $K^- K^+$ system produced in the reactions $\pi^- p \to K^- K^+ n$ and $\pi^+ n \to K^- K^+ p$ at 6-GeV/c, Phys. Rev. D **22**, 2595 (1980).
[14] J. H. Alvarenga Nogueira, I. Bediaga, A. B. R. Cavalcante, T. Frederico, and O. Lourenço, CP violation: Dalitz interference, CPT, and final state interactions, Phys. Rev. D **92**, 054010 (2015).
[15] L. Wolfenstein, Final state interactions and CP violation in weak decays, Phys. Rev. D **43**, 151 (1991).
[16] I. I. Bigi and A. I. Sanda, CP violation, Cambridge Monogr. Part. Phys., Nucl. Phys., Cosmol. **9**, 1 (2009).
[17] G. N. Fleming, Recoupling effects in the isobar model. 1. General formalism for three-Pion scattering, Phys. Rev. **135**, B551 (1964).
[18] D. Herndon, P. Soding, and R. J. Cashmore, Generalized isobar model formalism, Phys. Rev. D **11**, 3165 (1975).
[19] A. A. Alves Jr. *et al.*, The LHCb detector at the LHC, J. Instrum. **3**, S08005 (2008).
[20] R. Aaij *et al.* (LHCb Collaboration), LHCb detector performance, Int. J. Mod. Phys. A **30**, 1530022 (2015).
[21] T. Sjöstrand, S. Mrenna, and P. Skands, A brief introduction to PYTHIA 8.1, Comput. Phys. Commun. **178**, 852 (2008).
[22] I. Belyaev *et al.*, Handling of the generation of primary events in Gauss, the LHCb simulation framework, J. Phys. Conf. Ser. **331**, 032047 (2011).
[23] D. J. Lange, The EvtGen particle decay simulation package, Nucl. Instrum. Methods Phys. Res., Sect. A **462**, 152 (2001).
[24] P. Golonka and Z. Was, PHOTOS Monte Carlo: A precision tool for QED corrections in Z and W decays, Eur. Phys. J. C **45**, 97 (2006).
[25] J. Allison *et al.* (Geant4 Collaboration), Geant4 developments and applications, IEEE Trans. Nucl. Sci. **53**, 270 (2006); S. Agostinelli *et al.* (Geant4 Collaboration), Geant4: A simulation toolkit, Nucl. Instrum. Methods Phys. Res., Sect. A **506**, 250 (2003).
[26] M. Clemencic, G. Corti, S. Easo, C. R. Jones, S. Miglioranzi, M. Pappagallo, and P. Robbe, The LHCb simulation application, Gauss: Design, evolution and experience, J. Phys. Conf. Ser. **331**, 032023 (2011).
[27] M. Tanabashi *et al.* (Particle Data Group), Review of particle physics, Phys. Rev. D **98**, 030001 (2018).
[28] L. Breiman, J. H. Friedman, R. A. Olshen, and C. J. Stone, *Classification and Regression Trees* (Wadsworth International Group, Belmont, California, 1984).
[29] B. P. Roe, H.-J. Yang, J. Zhu, Y. Liu, I. Stancu, and G. McGregor, Boosted decision trees, an alternative to artificial neural networks, Nucl. Instrum. Methods Phys. Res., Sect. A **543**, 577 (2005).
[30] F. Archilli *et al.*, Performance of the muon identification at LHCb, J. Instrum. **8**, P10020 (2013).
[31] R. H. Dalitz, On the analysis of τ-meson data and the nature of the τ-meson, Philos. Mag. Ser. 7 **44**, 1068 (1953).

[32] J. M. Blatt and V. F. Weisskopf, *Theoretical Nuclear Physics* (Springer, New York, 1952).
[33] F. von Hippel and C. Quigg, Centrifugal-barrier effects in resonance partial decay widths, shapes, and production amplitudes, Phys. Rev. D **5**, 624 (1972).
[34] R. Aaij *et al.* (LHCb Collaboration), Dalitz plot analysis of $B_s^0 \to \bar{D}^0 K^- \pi^+$ decays, Phys. Rev. D **90**, 072003 (2014).
[35] B. Aubert *et al.* (*BABAR* Collaboration), Dalitz-plot analysis of the decays $B^\pm \to K^\pm \pi^\mp \pi^\pm$, Phys. Rev. D **72**, 072003 (2005); Erratum, Phys. Rev. D **74**, 099903 (2006).
[36] J. D. Jackson, Remarks on the phenomenological analysis of resonances, Nuovo Cimento **34**, 1644 (1964).
[37] J. Back *et al.*, LAURA^{++}: A Dalitz plot fitter, Comput. Phys. Commun. **231**, 198 (2018).
[38] E. Ben-Haim, R. Brun, B. Echenard, and T. E. Latham, JFIT: A framework to obtain combined experimental results through joint fits, arXiv:1409.5080.
[39] J. R. Pelaez and F. J. Yndurain, The pion-pion scattering amplitude, Phys. Rev. D **71**, 074016 (2005).
[40] R. Aaij *et al.* (LHCb Collaboration), Amplitude analysis of the $B^+ \to \pi^+\pi^+\pi^-$ decay, arXiv:1909.05212.
[41] R. Aaij *et al.* (LHCb Collaboration), Observation of several sources of CP violation in $B^+ \to \pi^+\pi^+\pi^-$ decays, arXiv:1909.05211.
[42] R. Aaij *et al.* (LHCb Collaboration), Measurement of CP asymmetry in $D^0 \to K^-K^+$ and $D^0 \to \pi^-\pi^+$ decays, J. High Energy Phys. 07 (2014) 041.

R. Aaij,[29] C. Abellán Beteta,[46] B. Adeva,[43] M. Adinolfi,[50] C. A. Aidala,[77] Z. Ajaltouni,[7] S. Akar,[61] P. Albicocco,[20] J. Albrecht,[12] F. Alessio,[44] M. Alexander,[55] A. Alfonso Albero,[42] G. Alkhazov,[35] P. Alvarez Cartelle,[57] A. A. Alves Jr.,[43] S. Amato,[2] S. Amerio,[25] Y. Amhis,[9] L. An,[19] L. Anderlini,[19] G. Andreassi,[45] M. Andreotti,[18] J. E. Andrews,[62] F. Archilli,[29] J. Arnau Romeu,[8] A. Artamonov,[41] M. Artuso,[63] K. Arzymatov,[39] E. Aslanides,[8] M. Atzeni,[46] B. Audurier,[24] S. Bachmann,[14] J. J. Back,[52] S. Baker,[57] V. Balagura,[9,b] W. Baldini,[18] A. Baranov,[39] R. J. Barlow,[58] S. Barsuk,[9] W. Barter,[57] M. Bartolini,[21] F. Baryshnikov,[73] V. Batozskaya,[33] B. Batsukh,[63] A. Battig,[12] V. Battista,[45] A. Bay,[45] J. Beddow,[55] F. Bedeschi,[26] I. Bediaga,[1] A. Beiter,[63] L. J. Bel,[29] S. Belin,[24] N. Beliy,[4] V. Bellee,[45] N. Belloli,[22,c] K. Belous,[41] I. Belyaev,[36] G. Bencivenni,[20] E. Ben-Haim,[10] S. Benson,[29] S. Beranek,[11] A. Berezhnoy,[37] R. Bernet,[46] D. Berninghoff,[14] E. Bertholet,[10] A. Bertolin,[25] C. Betancourt,[46] F. Betti,[17,44] M. O. Bettler,[51] Ia. Bezshyiko,[46] S. Bhasin,[50] J. Bhom,[31] M. S. Bieker,[12] S. Bifani,[49] P. Billoir,[10] A. Birnkraut,[12] A. Bizzeti,[19,d] M. Bjørn,[59] M. P. Blago,[44] T. Blake,[52] F. Blanc,[45] S. Blusk,[63] D. Bobulska,[55] V. Bocci,[28] O. Boente Garcia,[43] T. Boettcher,[60] A. Bondar,[40,e] N. Bondar,[35] S. Borghi,[58,44] M. Borisyak,[39] M. Borsato,[14] M. Boubdir,[11] T. J. V. Bowcock,[56] C. Bozzi,[18,44] S. Braun,[14] M. Brodski,[44] J. Brodzicka,[31] A. Brossa Gonzalo,[52] D. Brundu,[24,44] E. Buchanan,[50] A. Buonaura,[46] C. Burr,[58] A. Bursche,[24] J. Buytaert,[44] W. Byczynski,[44] S. Cadeddu,[24] H. Cai,[67] R. Calabrese,[18,f] R. Calladine,[49] M. Calvi,[22,c] M. Calvo Gomez,[42,g] A. Camboni,[42,g] P. Campana,[20] D. H. Campora Perez,[44] L. Capriotti,[17,h] A. Carbone,[17,h] G. Carboni,[27] R. Cardinale,[21] A. Cardini,[24] P. Carniti,[22,c] K. Carvalho Akiba,[2] G. Casse,[56] M. Cattaneo,[44] G. Cavallero,[21] R. Cenci,[26,i] M. G. Chapman,[50] M. Charles,[10] Ph. Charpentier,[44] G. Chatzikonstantinidis,[49] M. Chefdeville,[6] V. Chekalina,[39] C. Chen,[3] S. Chen,[24] S.-G. Chitic,[44] V. Chobanova,[43] M. Chrzaszcz,[44] A. Chubykin,[35] P. Ciambrone,[20] X. Cid Vidal,[43] G. Ciezarek,[44] F. Cindolo,[17] P. E. L. Clarke,[54] M. Clemencic,[44] H. V. Cliff,[51] J. Closier,[44] V. Coco,[44] J. A. B. Coelho,[9] J. Cogan,[8] E. Cogneras,[7] L. Cojocariu,[34] P. Collins,[44] T. Colombo,[44] A. Comerma-Montells,[14] A. Contu,[24] G. Coombs,[44] S. Coquereau,[42] G. Corti,[44] M. Corvo,[18,f] C. M. Costa Sobral,[52] B. Couturier,[44] G. A. Cowan,[54] D. C. Craik,[60] A. Crocombe,[52] M. Cruz Torres,[1] R. Currie,[54] F. Da Cunha Marinho,[2] C. L. Da Silva,[78] E. Dall'Occo,[29] J. Dalseno,[43,j] C. D'Ambrosio,[44] A. Danilina,[36] P. d'Argent,[14] A. Davis,[58] O. De Aguiar Francisco,[44] K. De Bruyn,[44] S. De Capua,[58] M. De Cian,[45] J. M. De Miranda,[1] L. De Paula,[2] M. De Serio,[16,k] P. De Simone,[20] J. A. de Vries,[29] C. T. Dean,[55] W. Dean,[77] D. Decamp,[6] L. Del Buono,[10] B. Delaney,[51] H.-P. Dembinski,[13] M. Demmer,[12] A. Dendek,[32] D. Derkach,[74] O. Deschamps,[7] F. Desse,[9] F. Dettori,[56] B. Dey,[68] A. Di Canto,[44] P. Di Nezza,[20] S. Didenko,[73] H. Dijkstra,[44] F. Dordei,[24] M. Dorigo,[44,l] A. C. dos Reis,[1] A. Dosil Suárez,[43] L. Douglas,[55] A. Dovbnya,[47] K. Dreimanis,[56] L. Dufour,[44] G. Dujany,[10] P. Durante,[44] J. M. Durham,[78] D. Dutta,[58] R. Dzhelyadin,[41,a] M. Dziewiecki,[14] A. Dziurda,[31] A. Dzyuba,[35] S. Easo,[53] U. Egede,[57] V. Egorychev,[36] S. Eidelman,[40,e] S. Eisenhardt,[54] U. Eitschberger,[12] R. Ekelhof,[12] L. Eklund,[55] S. Ely,[63] A. Ene,[34] S. Escher,[11] S. Esen,[29] T. Evans,[61] A. Falabella,[17] C. Färber,[44] N. Farley,[49] S. Farry,[56] D. Fazzini,[22,44,c] M. Féo,[44] P. Fernandez Declara,[44] A. Fernandez Prieto,[43] F. Ferrari,[17,h] L. Ferreira Lopes,[45] F. Ferreira Rodrigues,[2] M. Ferro-Luzzi,[44] S. Filippov,[38] R. A. Fini,[16] M. Fiorini,[18,f] M. Firlej,[32] C. Fitzpatrick,[45] T. Fiutowski,[32] F. Fleuret,[9,b] M. Fontana,[44] F. Fontanelli,[21,m] R. Forty,[44] V. Franco Lima,[56] M. Frank,[44] C. Frei,[44] J. Fu,[23,n] W. Funk,[44] E. Gabriel,[54] A. Gallas Torreira,[43] D. Galli,[17,h] S. Gallorini,[25] S. Gambetta,[54] Y. Gan,[3] M. Gandelman,[2] P. Gandini,[23] Y. Gao,[3] L. M. Garcia Martin,[76] J. García Pardiñas,[46]

B. Garcia Plana,[43] J. Garra Tico,[51] L. Garrido,[42] D. Gascon,[42] C. Gaspar,[44] G. Gazzoni,[7] D. Gerick,[14] E. Gersabeck,[58] M. Gersabeck,[58] T. Gershon,[52] D. Gerstel,[8] Ph. Ghez,[6] V. Gibson,[51] O. G. Girard,[45] P. Gironella Gironell,[42] L. Giubega,[34] K. Gizdov,[54] V. V. Gligorov,[10] C. Göbel,[65] D. Golubkov,[36] A. Golutvin,[57,73] A. Gomes,[1,o] I. V. Gorelov,[37] C. Gotti,[22,c] E. Govorkova,[29] J. P. Grabowski,[14] R. Graciani Diaz,[42] L. A. Granado Cardoso,[44] E. Graugés,[42] E. Graverini,[46] G. Graziani,[19] A. Grecu,[34] R. Greim,[29] P. Griffith,[24] L. Grillo,[58] L. Gruber,[44] B. R. Gruberg Cazon,[59] O. Grünberg,[70] C. Gu,[3] E. Gushchin,[38] A. Guth,[11] Yu. Guz,[41,44] T. Gys,[44] T. Hadavizadeh,[59] C. Hadjivasiliou,[7] G. Haefeli,[45] C. Haen,[44] S. C. Haines,[51] B. Hamilton,[62] X. Han,[14] T. H. Hancock,[59] S. Hansmann-Menzemer,[14] N. Harnew,[59] T. Harrison,[56] C. Hasse,[44] M. Hatch,[44] J. He,[4] M. Hecker,[57] K. Heinicke,[12] A. Heister,[12] K. Hennessy,[56] L. Henry,[76] M. Heß,[70] J. Heuel,[11] A. Hicheur,[64] R. Hidalgo Charman,[58] D. Hill,[59] M. Hilton,[58] P. H. Hopchev,[45] J. Hu,[14] W. Hu,[68] W. Huang,[4] Z. C. Huard,[61] W. Hulsbergen,[29] T. Humair,[57] M. Hushchyn,[74] D. Hutchcroft,[56] D. Hynds,[29] P. Ibis,[12] M. Idzik,[32] P. Ilten,[49] A. Inglessi,[35] A. Inyakin,[41] K. Ivshin,[35] R. Jacobsson,[44] S. Jakobsen,[44] J. Jalocha,[59] E. Jans,[29] B. K. Jashal,[76] A. Jawahery,[62] F. Jiang,[3] M. John,[59] D. Johnson,[44] C. R. Jones,[51] C. Joram,[44] B. Jost,[44] N. Jurik,[59] S. Kandybei,[47] M. Karacson,[44] J. M. Kariuki,[50] S. Karodia,[55] N. Kazeev,[74] M. Kecke,[14] F. Keizer,[51] M. Kelsey,[63] M. Kenzie,[51] T. Ketel,[30] E. Khairullin,[39] B. Khanji,[44] C. Khurewathanakul,[45] K. E. Kim,[63] T. Kirn,[11] V. S. Kirsebom,[45] S. Klaver,[20] K. Klimaszewski,[33] T. Klimkovich,[13] S. Koliiev,[48] M. Kolpin,[14] R. Kopecna,[14] P. Koppenburg,[29] I. Kostiuk,[29,48] S. Kotriakhova,[35] M. Kozeiha,[7] L. Kravchuk,[38] M. Kreps,[52] F. Kress,[57] P. Krokovny,[40,e] W. Krupa,[32] W. Krzemien,[33] W. Kucewicz,[31,p] M. Kucharczyk,[31] V. Kudryavtsev,[40,e] A. K. Kuonen,[45] T. Kvaratskheliya,[36,44] D. Lacarrere,[44] G. Lafferty,[58] A. Lai,[24] D. Lancierini,[46] G. Lanfranchi,[20] C. Langenbruch,[11] T. Latham,[52] C. Lazzeroni,[49] R. Le Gac,[8] R. Lefèvre,[7] A. Leflat,[37] F. Lemaitre,[44] O. Leroy,[8] T. Lesiak,[31] B. Leverington,[14] P.-R. Li,[4,q] Y. Li,[5] Z. Li,[63] X. Liang,[63] T. Likhomanenko,[72] R. Lindner,[44] F. Lionetto,[46] V. Lisovskyi,[9] G. Liu,[66] X. Liu,[3] D. Loh,[52] A. Loi,[24] I. Longstaff,[55] J. H. Lopes,[2] G. Loustau,[46] G. H. Lovell,[51] D. Lucchesi,[25,r] M. Lucio Martinez,[43] Y. Luo,[3] A. Lupato,[25] E. Luppi,[18,f] O. Lupton,[44] A. Lusiani,[26] X. Lyu,[4] F. Machefert,[9] F. Maciuc,[34] V. Macko,[45] P. Mackowiak,[12] S. Maddrell-Mander,[50] O. Maev,[35,44] K. Maguire,[58] D. Maisuzenko,[35] M. W. Majewski,[32] S. Malde,[59] B. Malecki,[44] A. Malinin,[72] T. Maltsev,[40,e] H. Malygina,[14] G. Manca,[24,s] G. Mancinelli,[8] D. Marangotto,[23,n] J. Maratas,[7,t] J. F. Marchand,[6] U. Marconi,[17] C. Marin Benito,[9] M. Marinangeli,[45] P. Marino,[45] J. Marks,[14] P. J. Marshall,[56] G. Martellotti,[28] M. Martinelli,[44] D. Martinez Santos,[43] F. Martinez Vidal,[76] A. Massafferri,[1] M. Materok,[11] R. Matev,[44] A. Mathad,[52] Z. Mathe,[44] C. Matteuzzi,[22] K. R. Mattioli,[77] A. Mauri,[46] E. Maurice,[9,b] B. Maurin,[45] M. McCann,[57,44] A. McNab,[58] R. McNulty,[15] J. V. Mead,[56] B. Meadows,[61] C. Meaux,[8] N. Meinert,[70] D. Melnychuk,[33] M. Merk,[29] A. Merli,[23,n] E. Michielin,[25] D. A. Milanes,[69] E. Millard,[52] M.-N. Minard,[6] L. Minzoni,[18,f] D. S. Mitzel,[14] A. Mödden,[12] A. Mogini,[10] R. D. Moise,[57] T. Mombächer,[12] I. A. Monroy,[69] S. Monteil,[7] M. Morandin,[25] G. Morello,[20] M. J. Morello,[26,u] O. Morgunova,[72] J. Moron,[32] A. B. Morris,[8] R. Mountain,[63] F. Muheim,[54] M. Mukherjee,[68] M. Mulder,[29] D. Müller,[44] J. Müller,[12] K. Müller,[46] V. Müller,[12] C. H. Murphy,[59] D. Murray,[58] P. Naik,[50] T. Nakada,[45] R. Nandakumar,[53] A. Nandi,[59] T. Nanut,[45] I. Nasteva,[2] M. Needham,[54] N. Neri,[23,n] S. Neubert,[14] N. Neufeld,[44] R. Newcombe,[57] T. D. Nguyen,[45] C. Nguyen-Mau,[45,v] S. Nieswand,[11] R. Niet,[12] N. Nikitin,[37] A. Nogay,[72] N. S. Nolte,[44] A. Oblakowska-Mucha,[32] V. Obraztsov,[41] S. Ogilvy,[55] D. P. O'Hanlon,[17] R. Oldeman,[24,s] C. J. G. Onderwater,[71] A. Ossowska,[31] J. M. Otalora Goicochea,[2] T. Ovsiannikova,[36] P. Owen,[46] A. Oyanguren,[76] P. R. Pais,[45] T. Pajero,[26,u] A. Palano,[16] M. Palutan,[20] G. Panshin,[75] A. Papanestis,[53] M. Pappagallo,[54] L. L. Pappalardo,[18,f] W. Parker,[62] C. Parkes,[58,44] G. Passaleva,[19,44] A. Pastore,[16] M. Patel,[57] C. Patrignani,[17,h] A. Pearce,[44] A. Pellegrino,[29] G. Penso,[28] M. Pepe Altarelli,[44] S. Perazzini,[44] D. Pereima,[36] P. Perret,[7] L. Pescatore,[45] K. Petridis,[50] A. Petrolini,[21,m] A. Petrov,[72] S. Petrucci,[54] M. Petruzzo,[23,n] B. Pietrzyk,[6] G. Pietrzyk,[45] M. Pikies,[31] M. Pili,[59] D. Pinci,[28] J. Pinzino,[44] F. Pisani,[44] A. Piucci,[14] V. Placinta,[34] S. Playfer,[54] J. Plews,[49] M. Plo Casasus,[43] F. Polci,[10] M. Poli Lener,[20] A. Poluektov,[8] N. Polukhina,[73,w] I. Polyakov,[63] E. Polycarpo,[2] G. J. Pomery,[50] S. Ponce,[44] A. Popov,[41] D. Popov,[49,13] S. Poslavskii,[41] E. Price,[50] J. Prisciandaro,[43] C. Prouve,[43] V. Pugatch,[48] A. Puig Navarro,[46] H. Pullen,[59] G. Punzi,[26,i] W. Qian,[4] J. Qin,[4] R. Quagliani,[10] B. Quintana,[7] N. V. Raab,[15] B. Rachwal,[32] J. H. Rademacker,[50] M. Rama,[26] M. Ramos Pernas,[43] M. S. Rangel,[2] F. Ratnikov,[39,74] G. Raven,[30] M. Ravonel Salzgeber,[44] M. Reboud,[6] F. Redi,[45] S. Reichert,[12] F. Reiss,[10] C. Remon Alepuz,[76] Z. Ren,[3] V. Renaudin,[59] S. Ricciardi,[53] S. Richards,[50] K. Rinnert,[56] P. Robbe,[9] A. Robert,[10] A. B. Rodrigues,[45] E. Rodrigues,[61] J. A. Rodriguez Lopez,[69] M. Roehrken,[44] S. Roiser,[44] A. Rollings,[59] V. Romanovskiy,[41] A. Romero Vidal,[43] J. D. Roth,[77] M. Rotondo,[20] M. S. Rudolph,[63] T. Ruf,[44] J. Ruiz Vidal,[76] J. J. Saborido Silva,[43] N. Sagidova,[35] B. Saitta,[24,s] V. Salustino Guimaraes,[65] C. Sanchez Gras,[29] C. Sanchez Mayordomo,[76] B. Sanmartin Sedes,[43] R. Santacesaria,[28] C. Santamarina Rios,[43] M. Santimaria,[20,44] E. Santovetti,[27,x] G. Sarpis,[58] A. Sarti,[20,y] C. Satriano,[28,z] A. Satta,[27] M. Saur,[4]

D. Savrina,[36,37] S. Schael,[11] M. Schellenberg,[12] M. Schiller,[55] H. Schindler,[44] M. Schmelling,[13] T. Schmelzer,[12] B. Schmidt,[44] O. Schneider,[45] A. Schopper,[44] H. F. Schreiner,[61] M. Schubiger,[45] S. Schulte,[45] M. H. Schune,[9] R. Schwemmer,[44] B. Sciascia,[20] A. Sciubba,[28,y] A. Semennikov,[36] E. S. Sepulveda,[10] A. Sergi,[49] N. Serra,[46] J. Serrano,[8] L. Sestini,[25] A. Seuthe,[12] P. Seyfert,[44] M. Shapkin,[41] T. Shears,[56] L. Shekhtman,[40,e] V. Shevchenko,[72] E. Shmanin,[73] B. G. Siddi,[18] R. Silva Coutinho,[46] L. Silva de Oliveira,[2] G. Simi,[25,r] S. Simone,[16,k] I. Skiba,[18] N. Skidmore,[14] T. Skwarnicki,[63] M. W. Slater,[49] J. G. Smeaton,[51] E. Smith,[11] I. T. Smith,[54] M. Smith,[57] M. Soares,[17] l. Soares Lavra,[1] M. D. Sokoloff,[61] F. J. P. Soler,[55] B. Souza De Paula,[2] B. Spaan,[12] E. Spadaro Norella,[23,n] P. Spradlin,[55] F. Stagni,[44] M. Stahl,[14] S. Stahl,[44] P. Stefko,[45] S. Stefkova,[57] O. Steinkamp,[46] S. Stemmle,[14] O. Stenyakin,[41] M. Stepanova,[35] H. Stevens,[12] A. Stocchi,[9] S. Stone,[63] B. Storaci,[46] S. Stracka,[26] M. E. Stramaglia,[45] M. Straticiuc,[34] U. Straumann,[46] S. Strokov,[75] J. Sun,[3] L. Sun,[67] Y. Sun,[62] K. Swientek,[32] A. Szabelski,[33] T. Szumlak,[32] M. Szymanski,[4] Z. Tang,[3] T. Tekampe,[12] G. Tellarini,[18] F. Teubert,[44] E. Thomas,[44] M. J. Tilley,[57] V. Tisserand,[7] S. T'Jampens,[6] M. Tobin,[32] S. Tolk,[44] L. Tomassetti,[18,f] D. Tonelli,[26] D. Y. Tou,[10] R. Tourinho Jadallah Aoude,[1] E. Tournefier,[6] M. Traill,[55] M. T. Tran,[45] A. Trisovic,[51] A. Tsaregorodtsev,[8] G. Tuci,[26,i] A. Tully,[51] N. Tuning,[29,44] A. Ukleja,[33] A. Usachov,[9] A. Ustyuzhanin,[39,74] U. Uwer,[14] A. Vagner,[75] V. Vagnoni,[17] A. Valassi,[44] S. Valat,[44] G. Valenti,[17] M. van Beuzekom,[29] E. van Herwijnen,[44] J. van Tilburg,[29] M. van Veghel,[29] R. Vazquez Gomez,[44] P. Vazquez Regueiro,[43] C. Vázquez Sierra,[29] S. Vecchi,[18] J. J. Velthuis,[50] M. Veltri,[19,aa] A. Venkateswaran,[63] M. Vernet,[7] M. Veronesi,[29] M. Vesterinen,[52] J. V. Viana Barbosa,[44] D. Vieira,[4] M. Vieites Diaz,[43] H. Viemann,[70] X. Vilasis-Cardona,[42,g] A. Vitkovskiy,[29] M. Vitti,[51] V. Volkov,[37] A. Vollhardt,[46] D. Vom Bruch,[10] B. Voneki,[44] A. Vorobyev,[35] V. Vorobyev,[40,e] N. Voropaev,[35] R. Waldi,[70] J. Walsh,[26] J. Wang,[5] M. Wang,[3] Y. Wang,[68] Z. Wang,[46] D. R. Ward,[51] H. M. Wark,[56] N. K. Watson,[49] D. Websdale,[57] A. Weiden,[46] C. Weisser,[60] M. Whitehead,[11] G. Wilkinson,[59] M. Wilkinson,[63] I. Williams,[51] M. Williams,[60] M. R. J. Williams,[58] T. Williams,[49] F. F. Wilson,[53] M. Winn,[9] W. Wislicki,[33] M. Witek,[31] G. Wormser,[9] S. A. Wotton,[51] K. Wyllie,[44] D. Xiao,[68] Y. Xie,[68] A. Xu,[3] M. Xu,[68] Q. Xu,[4] Z. Xu,[6] Z. Xu,[3] Z. Yang,[3] Z. Yang,[62] Y. Yao,[63] L. E. Yeomans,[56] H. Yin,[68] J. Yu,[68,bb] X. Yuan,[63] O. Yushchenko,[41] K. A. Zarebski,[49] M. Zavertyaev,[13,w] M. Zeng,[3] D. Zhang,[68] L. Zhang,[3] W. C. Zhang,[3,cc] Y. Zhang,[44] A. Zhelezov,[14] Y. Zheng,[4] X. Zhu,[3] V. Zhukov,[11,37] J. B. Zonneveld,[54] and S. Zucchelli[17,h]

(LHCb Collaboration)

[1]*Centro Brasileiro de Pesquisas Físicas (CBPF), Rio de Janeiro, Brazil*
[2]*Universidade Federal do Rio de Janeiro (UFRJ), Rio de Janeiro, Brazil*
[3]*Center for High Energy Physics, Tsinghua University, Beijing, China*
[4]*University of Chinese Academy of Sciences, Beijing, China*
[5]*Institute Of High Energy Physics (ihep), Beijing, China*
[6]*Univ. Grenoble Alpes, Univ. Savoie Mont Blanc, CNRS, IN2P3-LAPP, Annecy, France*
[7]*Université Clermont Auvergne, CNRS/IN2P3, LPC, Clermont-Ferrand, France*
[8]*Aix Marseille Univ, CNRS/IN2P3, CPPM, Marseille, France*
[9]*LAL, Univ. Paris-Sud, CNRS/IN2P3, Université Paris-Saclay, Orsay, France*
[10]*LPNHE, Sorbonne Université, Paris Diderot Sorbonne Paris Cité, CNRS/IN2P3, Paris, France*
[11]*I. Physikalisches Institut, RWTH Aachen University, Aachen, Germany*
[12]*Fakultät Physik, Technische Universität Dortmund, Dortmund, Germany*
[13]*Max-Planck-Institut für Kernphysik (MPIK), Heidelberg, Germany*
[14]*Physikalisches Institut, Ruprecht-Karls-Universität Heidelberg, Heidelberg, Germany*
[15]*School of Physics, University College Dublin, Dublin, Ireland*
[16]*INFN Sezione di Bari, Bari, Italy*
[17]*INFN Sezione di Bologna, Bologna, Italy*
[18]*INFN Sezione di Ferrara, Ferrara, Italy*
[19]*INFN Sezione di Firenze, Firenze, Italy*
[20]*INFN Laboratori Nazionali di Frascati, Frascati, Italy*
[21]*INFN Sezione di Genova, Genova, Italy*
[22]*INFN Sezione di Milano-Bicocca, Milano, Italy*
[23]*INFN Sezione di Milano, Milano, Italy*
[24]*INFN Sezione di Cagliari, Monserrato, Italy*
[25]*INFN Sezione di Padova, Padova, Italy*
[26]*INFN Sezione di Pisa, Pisa, Italy*

[27]*INFN Sezione di Roma Tor Vergata, Roma, Italy*
[28]*INFN Sezione di Roma La Sapienza, Roma, Italy*
[29]*Nikhef National Institute for Subatomic Physics, Amsterdam, Netherlands*
[30]*Nikhef National Institute for Subatomic Physics and VU University Amsterdam, Amsterdam, Netherlands*
[31]*Henryk Niewodniczanski Institute of Nuclear Physics Polish Academy of Sciences, Kraków, Poland*
[32]*AGH—University of Science and Technology, Faculty of Physics and Applied Computer Science, Kraków, Poland*
[33]*National Center for Nuclear Research (NCBJ), Warsaw, Poland*
[34]*Horia Hulubei National Institute of Physics and Nuclear Engineering, Bucharest-Magurele, Romania*
[35]*Petersburg Nuclear Physics Institute NRC Kurchatov Institute (PNPI NRC KI), Gatchina, Russia*
[36]*Institute of Theoretical and Experimental Physics NRC Kurchatov Institute (ITEP NRC KI), Moscow, Russia, Moscow, Russia*
[37]*Institute of Nuclear Physics, Moscow State University (SINP MSU), Moscow, Russia*
[38]*Institute for Nuclear Research of the Russian Academy of Sciences (INR RAS), Moscow, Russia*
[39]*Yandex School of Data Analysis, Moscow, Russia*
[40]*Budker Institute of Nuclear Physics (SB RAS), Novosibirsk, Russia*
[41]*Institute for High Energy Physics NRC Kurchatov Institute (IHEP NRC KI), Protvino, Russia, Protvino, Russia*
[42]*ICCUB, Universitat de Barcelona, Barcelona, Spain*
[43]*Instituto Galego de Física de Altas Enerxías (IGFAE), Universidade de Santiago de Compostela, Santiago de Compostela, Spain*
[44]*European Organization for Nuclear Research (CERN), Geneva, Switzerland*
[45]*Institute of Physics, Ecole Polytechnique Fédérale de Lausanne (EPFL), Lausanne, Switzerland*
[46]*Physik-Institut, Universität Zürich, Zürich, Switzerland*
[47]*NSC Kharkiv Institute of Physics and Technology (NSC KIPT), Kharkiv, Ukraine*
[48]*Institute for Nuclear Research of the National Academy of Sciences (KINR), Kyiv, Ukraine*
[49]*University of Birmingham, Birmingham, United Kingdom*
[50]*H.H. Wills Physics Laboratory, University of Bristol, Bristol, United Kingdom*
[51]*Cavendish Laboratory, University of Cambridge, Cambridge, United Kingdom*
[52]*Department of Physics, University of Warwick, Coventry, United Kingdom*
[53]*STFC Rutherford Appleton Laboratory, Didcot, United Kingdom*
[54]*School of Physics and Astronomy, University of Edinburgh, Edinburgh, United Kingdom*
[55]*School of Physics and Astronomy, University of Glasgow, Glasgow, United Kingdom*
[56]*Oliver Lodge Laboratory, University of Liverpool, Liverpool, United Kingdom*
[57]*Imperial College London, London, United Kingdom*
[58]*School of Physics and Astronomy, University of Manchester, Manchester, United Kingdom*
[59]*Department of Physics, University of Oxford, Oxford, United Kingdom*
[60]*Massachusetts Institute of Technology, Cambridge, Massachusetts, USA*
[61]*University of Cincinnati, Cincinnati, Ohio, USA*
[62]*University of Maryland, College Park, Maryland, USA*
[63]*Syracuse University, Syracuse, New York, USA*
[64]*Laboratory of Mathematical and Subatomic Physics, Constantine, Algeria*
[associated with Universidade Federal do Rio de Janeiro (UFRJ), Rio de Janeiro, Brazil]
[65]*Pontifícia Universidade Católica do Rio de Janeiro (PUC-Rio), Rio de Janeiro, Brazil*
[associated with Universidade Federal do Rio de Janeiro (UFRJ), Rio de Janeiro, Brazil]
[66]*South China Normal University, Guangzhou, China*
[associated with Center for High Energy Physics, Tsinghua University, Beijing, China]
[67]*School of Physics and Technology, Wuhan University, Wuhan, China*
[associated with Center for High Energy Physics, Tsinghua University, Beijing, China]
[68]*Institute of Particle Physics, Central China Normal University, Wuhan, Hubei, China*
[associated with Center for High Energy Physics, Tsinghua University, Beijing, China]
[69]*Departamento de Fisica, Universidad Nacional de Colombia, Bogota, Colombia*
(associated with LPNHE, Sorbonne Université, Paris Diderot Sorbonne Paris Cité, CNRS/IN2P3, Paris, France)
[70]*Institut für Physik, Universität Rostock, Rostock, Germany*
(associated with Physikalisches Institut, Ruprecht-Karls-Universität Heidelberg, Heidelberg, Germany)
[71]*Van Swinderen Institute, University of Groningen, Groningen, Netherlands*
(associated with Nikhef National Institute for Subatomic Physics, Amsterdam, Netherlands)
[72]*National Research Centre Kurchatov Institute, Moscow, Russia*
[associated with Institute of Theoretical and Experimental Physics NRC Kurchatov Institute (ITEP NRC KI), Moscow, Russia]
[73]*National University of Science and Technology "MISIS", Moscow, Russia*
[associated with Institute of Theoretical and Experimental Physics NRC Kurchatov Institute (ITEP NRC KI), Moscow, Russia]

[74]*National Research University Higher School of Economics, Moscow, Russia*
(associated with Yandex School of Data Analysis, Moscow, Russia)
[75]*National Research Tomsk Polytechnic University, Tomsk, Russia*
[associated with Institute of Theoretical and Experimental Physics NRC Kurchatov Institute (ITEP NRC KI), Moscow, Russia]
[76]*Instituto de Fisica Corpuscular, Centro Mixto Universidad de Valencia—CSIC, Valencia, Spain*
(associated with ICCUB, Universitat de Barcelona, Barcelona, Spain)
[77]*University of Michigan, Ann Arbor, USA*
(associated with Syracuse University, Syracuse, New York, USA)
[78]*Los Alamos National Laboratory (LANL), Los Alamos, USA*
(associated with Syracuse University, Syracuse, New York, USA)

[a]Deceased.
[b]Also at Laboratoire Leprince-Ringuet, Palaiseau, France.
[c]Also at Università di Milano Bicocca, Milano, Italy.
[d]Also at Università di Modena e Reggio Emilia, Modena, Italy.
[e]Also at Novosibirsk State University, Novosibirsk, Russia.
[f]Also at Università di Ferrara, Ferrara, Italy.
[g]Also at LIFAELS, La Salle, Universitat Ramon Llull, Barcelona, Spain.
[h]Also at Università di Bologna, Bologna, Italy.
[i]Also at Università di Pisa, Pisa, Italy.
[j]Also at H.H. Wills Physics Laboratory, University of Bristol, Bristol, United Kingdom.
[k]Also at Università di Bari, Bari, Italy.
[l]Also at Sezione INFN di Trieste, Trieste, Italy.
[m]Also at Università di Genova, Genova, Italy.
[n]Also at Università degli Studi di Milano, Milano, Italy.
[o]Also at Universidade Federal do Triângulo Mineiro (UFTM), Uberaba-MG, Brazil.
[p]Also at AGH—University of Science and Technology, Faculty of Computer Science, Electronics and Telecommunications, Kraków, Poland.
[q]Also at Lanzhou University, Lanzhou, China.
[r]Also at Università di Padova, Padova, Italy.
[s]Also at Università di Cagliari, Cagliari, Italy.
[t]Also at MSU—Iligan Institute of Technology (MSU-IIT), Iligan, Philippines.
[u]Also at Scuola Normale Superiore, Pisa, Italy.
[v]Also at Hanoi University of Science, Hanoi, Vietnam.
[w]Also at P.N. Lebedev Physical Institute, Russian Academy of Science (LPI RAS), Moscow, Russia.
[x]Also at Università di Roma Tor Vergata, Roma, Italy.
[y]Also at Università di Roma La Sapienza, Roma, Italy.
[z]Also at Università della Basilicata, Potenza, Italy.
[aa]Also at Università di Urbino, Urbino, Italy.
[bb]Also at Physics and Micro Electronic College, Hunan University, Changsha City, China.
[cc]Also at School of Physics and Information Technology, Shaanxi Normal University (SNNU), Xi'an, China.